Apparatus for the measurement of the speed of sound of ammonia up to high temperatures and pressures

Frithjof H. Dubberke[1], David B. Rasche[1], Elmar Baumhögger[1], and Jadran Vrabec[1, a)]

Lehrstuhl für Thermodynamik und Energietechnik, Universität Paderborn, Warburger Straße 100, 33098 Paderborn, Germany

(Dated: 11 August 2014)

An apparatus for the measurement of the speed of sound based on the pulse-echo technique is presented. It operates up to a temperature of 480 K and a pressure of 125 MPa. After referencing and validating the apparatus with water, it is applied to liquid ammonia between 230 and 410 K up to a pressure of 124 MPa. Speed of sound data are presented with an uncertainty between 0.02 and 0.1 %.

a)corresponding author, tel.: +49-5251/60-2421, fax: +49-5251/60-3522, email: jadran.vrabec@upb.de

I. INTRODUCTION

Ammonia is a ubiquitous compound due to its presence in many industrial processes and cleaning products. In addition to its classical applications in fermentation or fertilization, ammonia's properties allow for a good performance as a refrigerant or fuel. Due to the importance of ammonia, it is of great interest to have a very reliable model for its thermodynamic properties. Thermal pvT properties as well as heat capacity and speed of sound data in the homogenous fluid region, together with the vapor pressure and the saturated liquid density, form the basis of fundamental equations of state (EOS) that accurately describe the entire range of fluid states.

This work presents an apparatus for measuring the speed of sound at high temperatures and pressures to generate data for fluids that were insufficiently studied. The speed of sound of fluids can be measured in different ways. For gases, the spherical resonator is a suitable technique with a high accuracy that has been used e.g. by Beckermann and Kohler[1], Trusler and Zarari[2], Benedetto et al.[3], Mehl and Moldover[4,5] or Ewing et al.[6]. Another measurement principle for the speed of sound of liquids is based on the pulse-echo technique which was introduced in 1985 by Kortbeek et al.[7]. Among others, it was used by Gedanitz et al.[8], Ye et al.[9], Wang and Nur[10], Zak et al.[11], Benedetto et al.[12] or Meier and Kabelac[13].

Speed of sound measurements for ammonia have been carried out since the late 1960s, however, leaving a wide range of fluid states without data. In 1968, Blagoi et al.[14] published the first experimental results for the speed of sound of ammonia. These measurements were made for the liquid along the saturation line up to 270 K and 0.4 MPa. In the same year, Bowen and Thompson[15] published values for the adiabatic compressibility of liquid ammonia, derived from speed of sound measurements between the freezing point and the normal boiling point (from 196 to 240 K). It was not until 2007 that the speed of sound of ammonia was measured again. Estrada-Alexanders and Hurly[16] used an acoustic Greenspan viscometer to measure the kinematic viscosity and the speed of sound of several fluids, including ammonia. The covered temperature and pressure ranges were 0.22 to 3.38 MPa and 300 to 375 K, respectively. Finally, Abramson[17] published in 2008 results for the very high pressure regime of liquid ammonia. Using the impulsive stimulated scattering technique, speed of sound measurements up to 680 K and 3.75 GPa were made. In the present work, measurements were made in the temperature range from 230 to 410 K from somewhat above

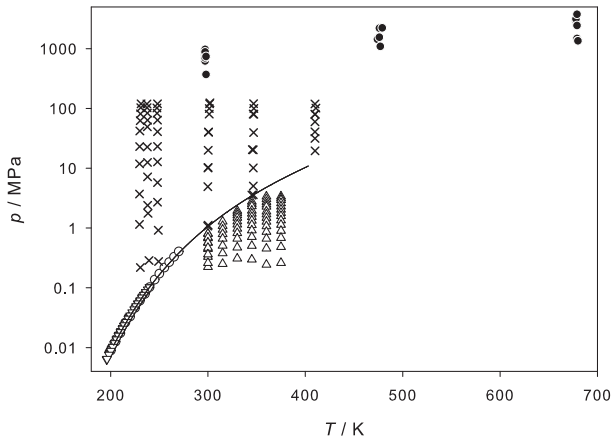

FIG. 1. Experimental speed of sound data for ammonia; ○ Blagoi et al. (1968); ▽ Bowen and Thompson (1988); △ Estrado-Alexanders and Hurly (2007); • Abramson (2008); × this work; —– saturation line

the saturation line up to 124 MPa, cf. Fig. 1.

II. APPARATUS

A. Construction

The measurement principle of the present apparatus is based on the pulse-echo technique with a double path length[8]. After emitting a high frequency modulated burst signal by a piezoelectric quartz crystal, which was positioned between two reflectors in the fluid, the speed of sound was determined by the time measurement of the signal propagation through the fluid. The ultrasonic sensor was identical with the one used by Gedanitz et al.[8].

The components of the measurement cell were made of stainless steel 1.4571 and were subjected to a heat treatment to remove self-stress from the manufacturing process. The piezoelectric quartz crystal was the main piece and was positioned between two polished reflectors. These reflectors were mounted with stainless steel screws $L_1 = 20$ mm above and $L_2 = 30$ mm below the quartz crystal, cf. Fig. 2. A X-cut crystal quartz was taken as a transducer which operated at a resonance frequency of 8 MHz. It was shaped as a circular

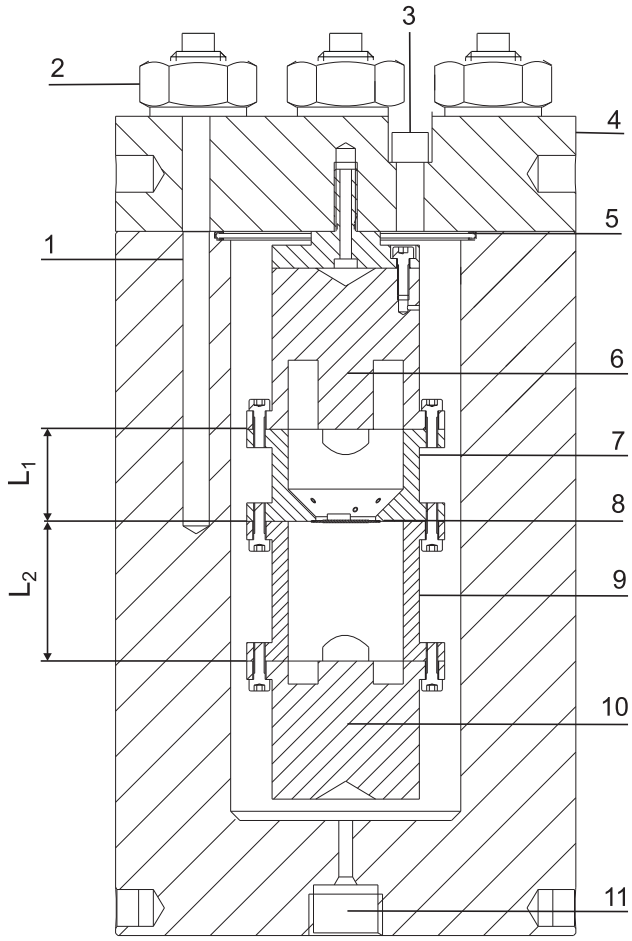

FIG. 2. Measuring cell in the pressure vessel: 1. thermometer seating, 2. fastening nuts, 3. safety outlet, 4. cell closure, 5. sealing ring, 6. reflector A, 7. path length L_1, 8. quartz, 9. path length L_2, 10. reflector B, 11. liquid sample inlet and outlet

disk with a diameter of 15 mm, having gold coated electrodes on both sides which measured 10 mm in diameter. Two clamps were connecting the electrodes, one to ground potential and the other one through a teflon coated wire to the control unit outside of the pressure vessel. The electrical feed through was realized by a glass insulation which was placed outside of the thermostat at the end of the inlet. This had the advantage that it was shielded against high temperatures and only had to withstand high pressures.

Fig. 3 shows the setup of the apparatus. In the center of the apparatus was the cell with the quartz crystal mounted in the pressure vessel. The pressure vessel had a cylindrical shape with an internal diameter of 50 mm and a wall thickness of 25 mm. It was made of highly tensile steel of type 1.4462. The sealing was done by a copper seal, supported by a rib

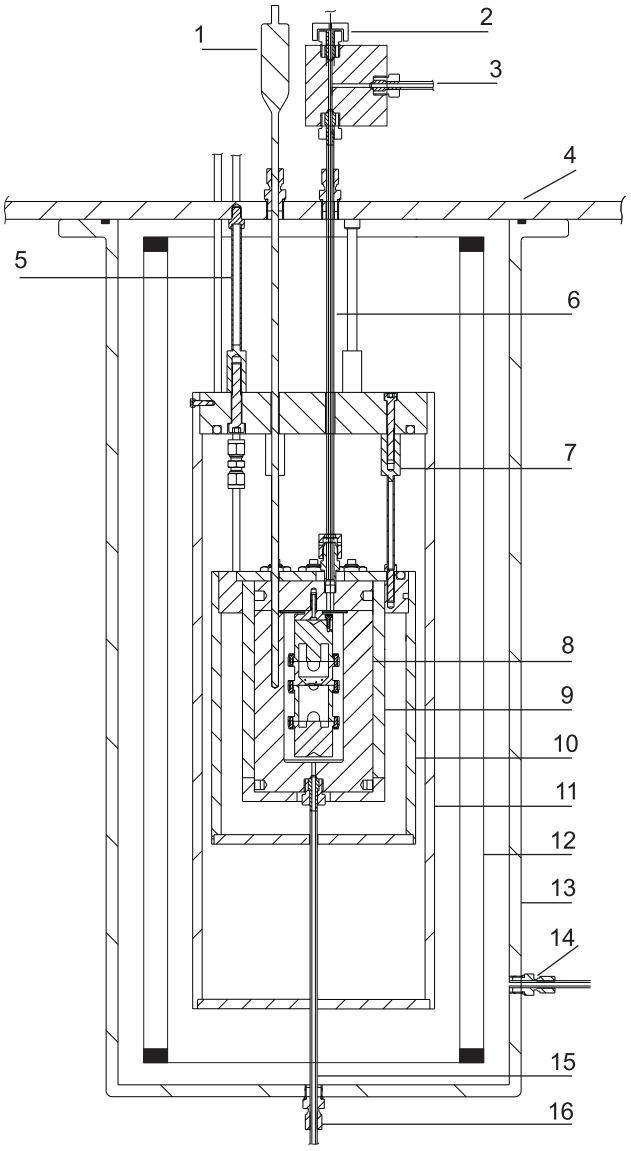

FIG. 3. Setup of the apparatus: 1. PT-100 thermometer, 2. electrical feed through, 3. safety outlet / burst disc, 4. base plate, 5. distance holder, 6. safety outlet / cable passage, 7. distance holder, 8. pressure vessel, 9. inner copper shielding, 10. central copper shielding, 11. outer copper shielding, 12. aluminum foils, 13. vacuum tank, 14. vacuum tank outlet, 15. liquid sample inlet and outlet, 16. vacuum sealing

profile which was milled into the surface of the sealing setting (note that dry ammonia with a water content of less than 400 ppm does not react with copper[18]). The pressure vessel itself was girded and fixed by a copper jacket to yield a uniform temperature distribution. This copper jacket was surrounded by two larger copper shieldings, each equipped with

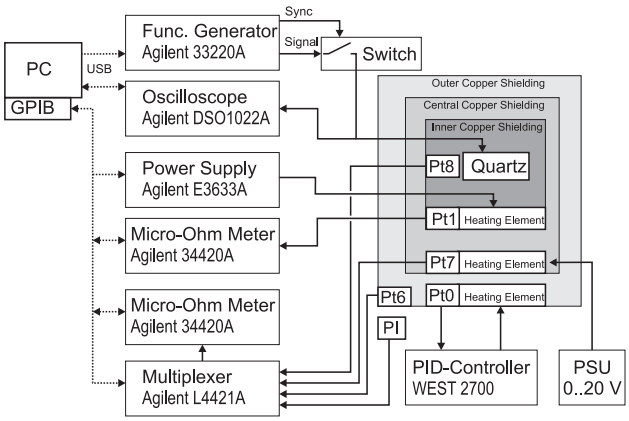

FIG. 4. Arrangement of electronic devices for temperature control, pressure measurement as well as signal generation and detection

a heating unit of 150 W electrical power for thermostating. Four layers of aluminum foil around the outer copper shielding reduced heat loss due to thermal radiation. Finally, the whole device was placed into a vacuum tank to reduce heat loss due to convection. Above the outer copper shielding, an aluminum plate was mounted to shield the cables and the electronic devices outside of the vacuum tank from thermal stress. The entire apparatus was mounted below an aluminum plate that was attached to the base frame of the test rig. The hanging construction was advantageous because of the good accessibility of the cell in case of maintenance. Heat loss through thermal conduction was minimized by contacting the acoustic sensor with the environment only by three distance holders of stainless steel that were attached to the central copper shielding, which was again contacted to the base plate by three other distance holders. The vacuum tank was about 420 mm in diameter and 1100 mm in height and was sealed with rubber. It had an inlet / outlet at the bottom for liquid samples, leading straight to the measuring cell, and another opening on the side for a connection to a vacuum pump. Three additional openings were at the retaining plate for the safety outlet, for the thermometers as well as an electrical feed trough for the cables of the heating elements and the temperature sensors.

B. Temperature

For controlling the cell with a high accuracy over a wide range of temperature, the thermostat was constructed with three copper shields. Each was monitored with respect to

the temperature and equipped with one independently adjustable heater, cf. Fig. 4. The temperature of the liquid was measured with a PT-100 thermometer (Rössel Messtechnik RM-type) mounted in the wall of the pressure cylinder next to the quartz, i.e. Pt8 in Fig. 4. The inner copper shielding was heated with a Thermocoax heating element and monitored with Pt1, cf. Fig. 4.

The control mode of the inner heating element is shown in Fig. 5. To quickly specify a constant temperature at the quartz without overshooting, a combination of a PID controller and an additional proportional (P) controller was used. Both were implemented in the control computer software. The PID controller provided the temperature control at the inner heater with its sensor Pt1 that was very close to the heating element. To reach the specified temperature at the quartz, the set point of the PID controller was calculated from the difference of the temperature measured by Pt8 and its set point. To prevent overshooting, the set point of the PID controller was limited to an adjustable range around the set point of Pt8. This proportional control algorithm leads to a small deviation which can be minimized by adding it to the set point to accurately reach the specified temperature. The outer copper shielding had another heating element which was adjusted manually with the help of a PID controller to 2 K below the desired fluid temperature. A supporting heating element, with the only purpose to boost heating, was attached to the second shielding and was regulated by a manual adjustment of a 12 V power supply. To monitor and control the cell temperature, a multiplexer (Agilent L4421A), two $\mu\Omega$-meters (Agilent 34420A) and a programmable power supply (Agilent E3633A) were connected to the computer via a GPIB interface. The heating loop had an accuracy of $\pm$ 3 mK around the specified fluid temperature, cf. Fig. 6.

The calibration of the Pt8 (PT 100/0) thermometer was done with a standardized 25 Ω platinum thermometer (Rosemount 162 CE) which was calibrated from 84 to 693 K at the Physikalisch-Technische Bundesanstalt in Braunschweig with an given uncertainty of 2.5 mK[19]. Calibration of Pt8 took place from 290 to 650 K. The uncertainty of the temperature measurement consisted of the uncertainty of the thermometer calibration (10 mK), the uncertainty of the measurement of the resistance ratio (2 mK), the stability of the temperature in the thermostat (4 mK, operating experience) and the inhomogeneity of the temperature field inside the pressure vessel. For resistance measurement, a $\mu\Omega$-meter (Agilent 34420A) was used, which was validated against a standard 100 Ω resistor (H. Tinsley & Co 5685 A) with a given uncertainty of 27 mK drift per year. Hence, the overall

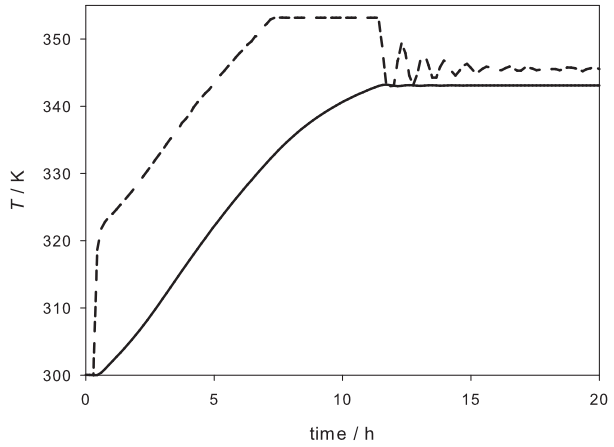

FIG. 5. Temperature control of the heating element. Solid line: cell temperature; dashed line: heating element temperature

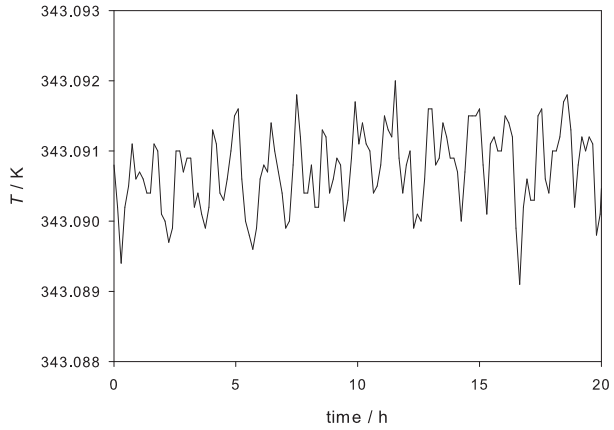

FIG. 6. Cell temperature reading via Pt8

uncertainty of the temperature measurement results according to the error propagation due the individual uncertainty contributions to $u_{\Delta T} = 30$ mK.

C. Pressure

The piping system is shown in Fig. 7. It was used to fill the cell with the liquid sample and to specify the pressure. Important components of the pressure system were an upper safety outlet of the pressure vessel, giving the possibility to create a vacuum inside the pressure vessel, a liquid sample container at the end of the inlet and a hand pump to adjust

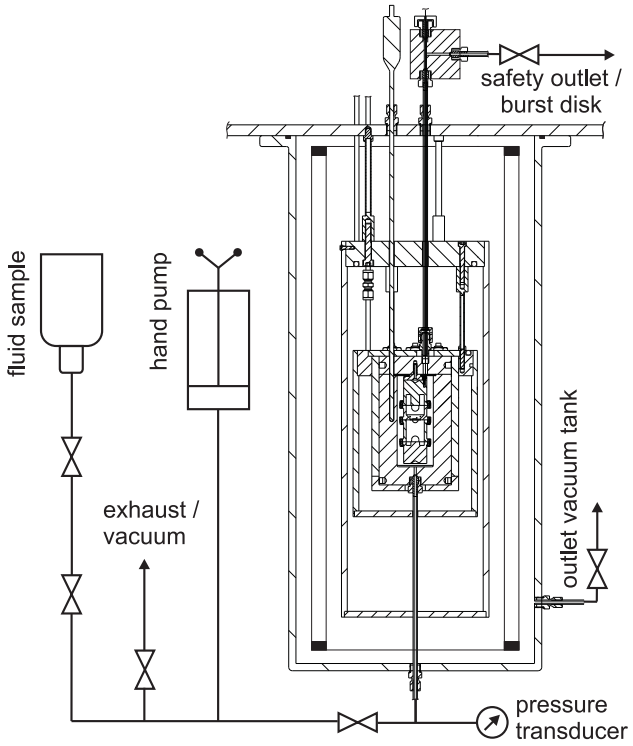

FIG. 7. Schematic of the pressure system

the pressure. Before filling the cell with a liquid, a vacuum was created. Subsequently, the liquid sample was imbibed into the cell. For an accurate pressure adjustment, a hand pump (HIP 50-5.75-30) was used. To achieve higher pressure levels, it was necessary to add more liquid into the cell. To this end, two valves were used to refill the hand pump without pressure loss in the cell.

The pressure was measured with a transducer (Honeywell TJE with a measuring range from 0 to 200 MPa and an accuracy of $\pm 0.1\%$ with respect to the full scale), which was protected by a blowout disc in case of overpressure. A $\mu\Omega$-meter (Agilent 34420A) was employed to measure the signal to supply voltage ratio. All pressurized components were connected via high pressure stainless steel tubes. The pressure transducer was calibrated with a dead weight tester (DH-Budenberg 580 EHX) for measurements up to 260 MPa with a specified uncertainty of 0.04 % of its full scale. All valves (HIP 30.000 psi) were chosen to withstand operating pressures of up to 206 MPa. The maximum shear stress test of the pressure vessel was at about 190 MPa.

D. Signal

An arbitrary function generator (Agilent 33220A) was used to generate the burst signal and an oscilloscope (Agilent DSO1022A) was used as a detecting device, cf. Fig. 4. Both were connected to the control computer via a USB interface. The switch, which was triggered via the function generator sync output, transmitted the burst signal to the quartz crystal and its subsequent echoes to the oscilloscope. Coaxial cables with an impedance of 50 Ω were employed to connect the signal components. To compensate the capacitance of the quartz crystal, a variable inductance was placed into the circuit.

III. VALIDATION AND REFERENCING

Water is available at high purity and highly accurate speed of sound measurements have been done for this substance over a wide range of states. The referencing of the path length distance $\Delta L = L_2 - L_1$ was thus carried out with water following Gedanitz et al.[8]. Furthermore, a comparison of the speed of sound measurements at high temperatures and high pressures was done with recently published data by Lin and Trusler[20], because the uncertainty of the EOS by Wagner and Pruss[21] increases significantly for $T \geq 300$ K and $p \geq 100$ MPa to approximately 1 %. Fig. 8 illustrates speed of sound measurements for two isotherms for water from this work and from Lin and Trusler[20] (with a given relative uncertainty of less than 0.04 %) in comparison to the EOS[21] that is recommended by the International Association for the Properties of Water and Steam (IAPWS). These data show that the present apparatus operated reliably also at high temperatures and pressures.

IV. OPERATION PROCEDURE

After filling the liquid into the pressure vessel, an equilibration time of around 60 min to reach a constant pressure level was required. Subsequently, the quartz crystal was excited with a burst signal of 20 cycles, typically with a voltage of 10 V peak-to-peak, using the function generator. The two echoes, due to the reflections on both sides of the measuring cell, were loaded and stored into the computer via the oscilloscope and then identified via thresholds with an adjustable magnitude. To obtain an undistorted signal, a Fast Fourier Transform (FFT) algorithm was used[22]. Band path filtering with zero padding lesd to a

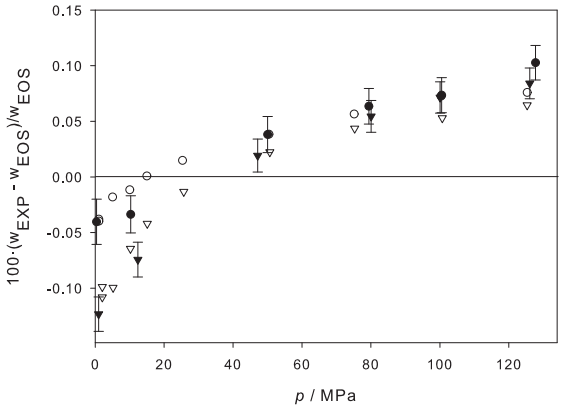

FIG. 8. Deviation of experimental speed of sound data from the EOS for water by Wagner and Pruss[21]: ○ 413 K, Lin and Trusler[20]; ● 413 K, this work; ▽ 473 K, Lin and Trusler[20]; ▼ 473 K, this work

high resolution in time and voltage amplitude as well as to a low random noise level. The time difference Δt, resulting from the path length difference $\Delta L = L_2 - L_1$, was calculated. Straightforwardly, the speed of sound is given then by

$$w = \frac{2\Delta L}{\Delta t}. \tag{1}$$

This equation does not consider diffraction, due to the phase shift of the signal relative to a planar propagation through the fluid, and dispersion effects leading to an uncertainty of the time difference Δt. The experimental speed of sound data were corrected by the diffraction correction by Harris[23], whereas significant dispersion effects did not occur for a resonance frequency of 8 MHz[24]. Furthermore, there was an uncertainty of the path length difference $\Delta L(T, p)$ from the referencing procedure with pure water and the measurement itself. The correction of the path length variation due to temperature and pressure was done with the following equation, where $\Delta L(T_0, p_0)$ is the path length difference at $T_0 = 293.15$ K and $p_0 = 0.1$ MPa

$$\Delta L(T, p) = \Delta L(T_0, p_0) \cdot \left[1 + \alpha(T - T_0) + \frac{1}{E}(1 - 2\nu)(p - p_0)\right]. \tag{2}$$

Parameters of the steel material 1.4571 are the linear thermal expansion coefficient α, the elastic modulus E and the poisson number ν, which were provided by steel supplier ThyssenKrupp Materials International (Werkstoffblatt 1.4571). Since two of these parame-

ters (α and E) are temperature dependent, the thermal expansion is given by a fourth-order polynomial and the mechanical expansion by a first-order polynomial. The resulting speed of sound uncertainty due to the steel parameters was estimated to be negligible with $6 \cdot 10^{-5}$ %.

V. RESULTS AND DISCUSSION

Measurements were made for ammonia as provided by Air Liquide ($N50$) with a given impurity of less than 8 ppm for a set of six isotherms, cf. Fig. 9. Starting somewhat above the vapor pressure, several measurements were made along each isotherm for different pressures up to 124 MPa. After each isotherm, the pressure was released and the measuring cell was refilled and pressurized with fresh ammonia.

The uncertainty of the present measurements is larger for lower pressures mainly due to the uncertainty of the pressure sensor. The measuring range of the pressure sensor was up to 200 MPa with an accuracy of $\pm 0.1\%$ of the full scale and therefore had an absolute uncertainty of 0.2 MPa. This uncertainty had the largest impact at high temperatures and low pressures, cf. Figs. 9 and 10. The overall speed of sound measurement uncertainty (u_w) is composed of the relevant contributions due to uncertainties of temperature ($u_{w,\Delta T}$) and pressure measurements ($u_{w,\Delta p}$), as well the uncertainty of the referencing procedure (u_{Ref}) and the uncertainty of the path length difference ($u_{\Delta L}$)

$$u_w = \sqrt{{u_{w,\Delta T}}^2 + {u_{w,\Delta p}}^2 + {u_{Ref}}^2 + {u_{\Delta L}}^2}. \tag{3}$$

The uncertainty of the operation procedure was limited by the internal time reference of the function generator and was thus neglected. According to the error propagation law, the uncertainty due to the referencing process and path length difference was 0.012 %. However, the total uncertainty increased up to 0.3 % for measurements at 346 and 410 K below 60 MPa. This increase is due to the fact that the relative uncertainty of the pressure measurement was significantly higher at low pressures combined with the high isothermal compressibility of the fluid at such thermodynamic states. For the remaining state points the total uncertainty varied between 0.02 to 0.1 %. Table 1 provides the present data together with their uncertainties.

The obtained speed of sound values were compared with the EOS by Tillner-Roth et al.[25].

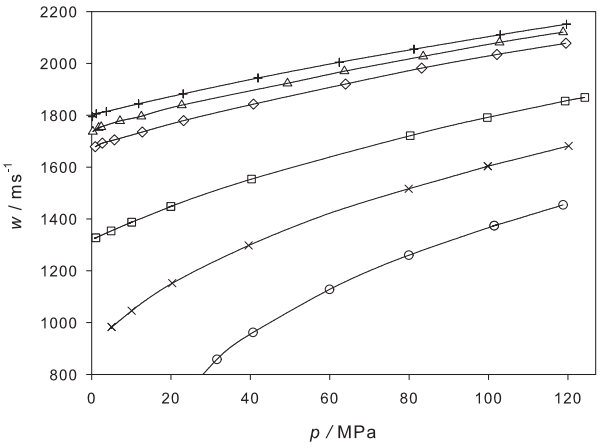

FIG. 9. Absolute values of the present speed of sound measurements along six isotherms: + 230 K; △ 237 K; ◊ 248 K; □ 300 K; × 346 K; ○ 410 K

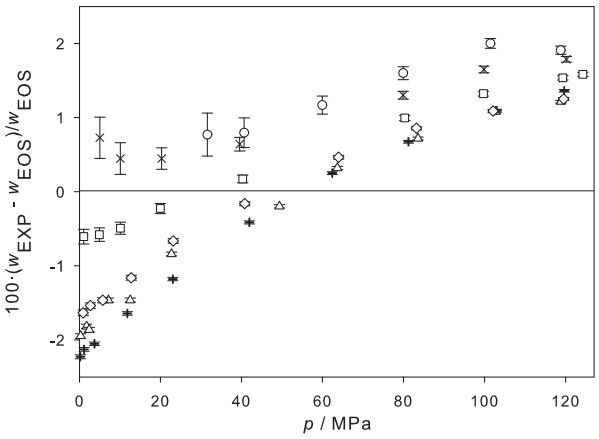

FIG. 10. Deviation of the present speed of sound measurements from the EOS by Tillner-Roth et al.[25]: + 230 K; △ 237 K; ◊ 248 K; □ 300 K; × 346 K; ○ 410 K

Observing the deviation from the experimental data, the accuracy of the EOS was assessed in the liquid state over a wide range of temperature and pressure, cf. Fig. 10. The uncertainty of the EOS for the speed of sound was specified by Tillner-Roth et al.[25] to be 2 %, except for the critical region where it was not further defined. This 2 % claim was confirmed here.

VI. CONCLUSION

An apparatus for the measurement of the speed of sound of liquids using the pulse-echo technique was built and validated with water by comparing the results with an accurate EOS for water and recently published experimental data by Lin and Trusler[20]. The speed of sound of ammonia was measured here for six isotherms from 273.15 to 410 K from somewhat above the vapor pressure up to 124 MPa. The measured speed of sound data for ammonia were compared with the EOS by Tillner-Roth et al.[25] and it was confirmed that the maximum deviation of the EOS is about 2 %.

This work covered a wide range of temperature and pressure in the liquid state for which no experimental data were available for ammonia. The present results show that the pulse-echo technique is a reliable and accurate method for the measurement of the speed of sound of liquid ammonia.

ACKNOWLEDGMENTS

The authors gratefully acknowledge the support of Holger Gedanitz and the assistance of Carlos Guillermo la Rubia García during the measurements.

REFERENCES

[1] W. Beekermann and F. Kohler, International Journal of Thermophysics **16**, 455 (1995).

[2] J. P. M. Trusler and M. Zarari, Journal of Chemical Thermodynamics **24**, 973 (1992).

[3] G. Benedetto, R. M. Gavioso, and R. Spagnolo, Rivista del Nuovo Cimento **22**, 1 (1999).

[4] J. B. Mehl and M. R. Moldover, Journal of Chemical Physics **74**, 4062 (1981).

[5] J. B. Mehl and M. R. Moldover, Journal of Chemical Physics **77**, 455 (1982).

[6] M. B. Ewing, A. R. H. Goodwin, M. L. McGlashan, and J. P. M. Trusler, Journal of Chemical Thermodynamics **19**, 721 (1987).

[7] P. J. Kortbeek, M. J. P. Muringer, N. J. Trappeniers, and S. N. Biswas, Review of Scientific Instruments **56**, 1269 (1985).

[8] H. Gedanitz, M. Davila, E. Baumhögger and R. Span, Journal of Chemical Thermodynamics **42**, 478 (2010).

[9]S. Ye, J. Alliez, B. Lagourette, H. Saint-Guirons, J. Arman, and P. Xans, Revue de Physique Appliquée **25**, 555 (1990).

[10]Z. Wang and A. Nur, Journal of the Acoustical Society of America **89**, 2725 (1991).

[11]A. Zak, M. Dzida, M. Zorebski, and A. Ernst, Review of Scientific Instruments **71**, 1756 (2000).

[12]G. Benedetto, R. M. Gavioso, P. A. G. Albo, S. Lago, D. M. Ripa, and R. Spagnolo, International Journal of Thermophysics **26**, 1651 (2005).

[13]K. Meier and S. Kabelac, Review of Scientific Instruments **77**, 123903 (2006).

[14]Y. P. Blagoi, A. E. Butko, S. Mikhailenko, and V. V. Yakuba, Russian Journal of Physical Chemistry, USSR **42**, 564 (1968).

[15]D. E. Bowen and J. C. Thompson, Journal of Chemical and Engineering Data **13**, 206 (1968).

[16]A. Estrada-Alexanders and J. Hurly, Journal of Chemical Thermodynamics **40**, 193 (2008).

[17]E. Abramson, Journal of Chemical and Engineering Data **53**, 1986 (2008).

[18]Refrigerants - Requirements and Symbols - Ref. Nr. DIN 8960 : 1998-11, Normenausschuss Kältetechnik (FNKä) (1998).

[19]Physikalisch-Technische Bundesanstalt, http://www.ptb.de/.

[20]C.-W. Lin and J. P. M. Trusler, Journal of Chemical Physics **136**, 094511 (2012).

[21]W. Wagner and A. Pruß, Journal of Physical and Chemical Reference Data **31**, 387 (2002).

[22]G. Benedetto, R. M. Gavioso, P. A. G. Albo, S. Lago, D. M. Ripa, and R. Spagnolo, International Journal of Thermophysics **26**, 1667 (2005).

[23]G. R. Harris, J. Acoust. Soc. Am. **70**, 10 (1981).

[24]K. Meier, *The Pulse-echo Method for High Precision Measurements of the speed of sound in Fluids* (University of the Federal Armed Forces, Hamburg, 2006).

[25]R. Tillner-Roth, F. Harms-Watzenberg, and H. D. Baehr, DKV-Tagungsbericht **20**, 167 (1993).

TABLE I. Experimental speed of sound data for ammonia, this work. The uncertainty of the pressure was throughout $\Delta p = 0.2$ MPa, the uncertainty of the speed of sound Δw is given for each state point individually.

T	p	w	Δw
[K]	[MPa]	[m/s]	[m/s]
230.61	0.2	1794.3	0.62
229.64	1.2	1805.8	0.61
229.64	3.7	1814.5	0.60
229.71	11.8	1844.3	0.58
229.8	23.1	1882.5	0.55
229.99	41.9	1943.9	0.51
230.37	62.4	2004.1	0.49
230.65	81.2	2054.9	0.47
230.99	103	2110.7	0.46
231.35	119.7	2151.2	0.45
239.44	0.3	1737	0.71
238.37	1.8	1751.8	0.69
238.1	2.4	1755	0.68
237.98	7.2	1778.3	0.66
237.83	12.5	1796	0.64
237.65	22.7	1839	0.60
237.8	49.4	1923.4	0.54
237.84	63.7	1970	0.52
237.75	83.6	2027.2	0.49
237.48	102.8	2081	0.48
237.37	118.8	2120.8	0.46
248.91	0.9	1678.4	0.79
248.1	2.7	1692.5	0.77
248.08	5.8	1705.2	0.75
248.05	12.8	1735.7	0.72
248.06	23.2	1779.2	0.67
248.13	40.8	1842.9	0.61
248.19	64	1920.4	0.56
247.65	83.2	1981.7	0.53
247.56	102.1	2034.4	0.50
248.07	119.5	2077.6	0.49

TABLE I. continued

T [K]	p [MPa]	w [m/s]	Δw [m/s]
299.72	1.1	1327	1.48
299.89	4.9	1354	1.38
300.02	10.1	1388	1.27
300.2	20	1448	1.11
300.5	40.3	1553.6	0.91
301.21	80.3	1721.1	0.70
301.34	99.7	1791.4	0.64
301.55	119.3	1855	0.60
302.03	124.3	1868.5	0.59
345.08	3.6	979	2.88
346.56	5	983	2.37
346.63	10.1	1046	1.79
346.47	20.3	1152	1.28
346.75	39.6	1298	0.87
347.07	79.9	1516.4	0.86
347.12	99.8	1603.5	0.77
346.85	120.2	1681.5	0.69
409.89	31.6	858	1.99
409.85	40.7	962	1.42
409.88	59.9	1128	1.13
409.89	79.9	1260	1.13
410.89	101.4	1374	0.94
409.92	118.8	1454.1	0.84